Available online at www.sciencedirect.com
ScienceDirect
Trans. Nonferrous Met. Soc. China 26(2016) 1574−1582
Transactions of Nonferrous Metals Society of China
www.tnmsc.cn

Microstructure, mechanical and bio-corrosion properties of as-extruded Mg−Sn−Ca alloys

Chao-yong ZHAO[1], Fu-sheng PAN[1,2,3], Hu-cheng PAN[4]

1. College of Materials Science and Engineering, Chongqing University, Chongqing 400044, China;
2. National Engineering Research Center for Magnesium Alloys, Chongqing University, Chongqing 400044, China;
3. Chongqing Academy of Science and Technology, Chongqing 401123, China;
4. Key Laboratory for Anisotropy and Texture of Materials, Ministry of Education, Northeastern University, Shenyang 110819, China;

Received 29 June 2015; accepted 25 February 2016

Abstract: The as-extruded Mg−Sn−Ca alloys were prepared and investigated for orthopedic applications via using optical microscopy, scanning electron microscopy, X-ray diffraction, as well as tensile, immersion and electrochemical tests. The results showed that, with the addition of 1% Sn and the Ca content of 0.2%−0.5%, the microstructure of the as-extruded Mg−Sn−Ca alloys became homogenous, which led to increased mechanical properties and improved corrosion resistance. Further increase of Ca content up to 1.5% improved the strength, but deteriorated the ductility and corrosion resistance. For the alloy containing 0.5% Ca, when the Sn content increased from 1% to 3%, the ultimate tensile strength increased with a decreased corrosion resistance, and the lowest yield strength and ductility appeared with the Sn content of 2%. These behaviors were determined by Sn/Ca mass ratio. The analyses showed that as-extruded Mg−1Sn−0.5Ca alloy was promising as a biodegradable orthopedic implant.

Key words: magnesium alloy; Mg−Sn−Ca alloy; biodegradation; orthopedic implant; microstructure; mechanical properties; corrosion

1 Introduction

Researches on magnesium and its alloys for orthopedic applications have increased significantly in recent years, due to their similar density and elastic modulus to cortical bone, good biocompatibility and biodegradability [1−4]. However, the low mechanical strength of magnesium and the rapid corrosion rate of magnesium alloys hindered their clinic use. Alloying is one of the most effective approaches to improve both mechanical properties and corrosion resistance of magnesium alloys, such as Mg−Al and/or RE alloy systems [2]. Although many studies reported that these alloys did not show toxicity in a short term [5−7], aluminum is well-known as a neurotoxicant, and the administration of some rare earths had potential toxical effect [8,9]. For biomedical application, biocompatibility of alloying elements must be taken into consideration during composition design [10].

Calcium (Ca) is naturally present in human bone and also essential in chemical signaling with cells [11]. The co-releasing of Mg and Ca ions was reported to be beneficial for bone healing [12]. In addition, Ca had a grain refining effect on Mg, and the addition of Ca into Mg usually formed Mg_2Ca intermetallic phase along grain boundaries due to the low solubility of Ca in Mg [13]. The corrosion rate of Mg−Ca alloys was closely related to the amount of Mg_2Ca phase [13,14]. Many studies demonstrated that Mg−Ca alloys with Ca addition less than 1.0% exhibited appropriate mechanical properties, low corrosion rate and good in vitro and in vivo biocompatibility [12,15,16]. However, the yield strength and the elongation of Mg−Ca alloy were needed to be further improved for the load-bearing application [12]. On the other hand, it was reported that the addition of Ca into magnesium alloys could improve mechanical properties and the corrosion resistance of the

Foundation item: Project (2013CB632200) supported by the National Basic Research Program of China; Projects (51474043, 51531002) supported by the National Natural Science Foundation of China; Projects (CSTC2013JCYJC60001, KJZH14101) supported by Chongqing Municipal Government, China; Project (2015M581350) supported by the China Postdoctoral Science Foundation
Corresponding author: Fu-sheng PAN; Tel: +86-23-65112635; E-mail: fspan@cqu.edu.cn
DOI: 10.1016/S1003-6326(16)64232-2

alloy [17,18]. Sn is present in the human body as one of the most essential elements, and it has been selected as the safe element for living body to prepare titanium alloys for biomedical applications [19]. A recent study conjectured that Sn might be a good alloying element for orthopedic magnesium alloy implants [10]. Furthermore, it was reported that simultaneous addition of Sn and Sr could obviously improve the corrosion resistance of magnesium alloys [20].

At present, although there were some reports about the as-cast and as-extruded Mg−Sn−Ca alloys for industrial applications [21−23], the research about as-extruded Mg−Sn−Ca alloys for orthopedic applications was scarce. In this study, Ca and Sn were selected as alloying elements for Mg to prepare the as-extruded Mg−Sn−Ca alloys for orthopedic applications, and the effects of Ca and Sn on the microstructure, mechanical and bio-corrosion properties of the as-extruded Mg−Sn−Ca alloys were investigated.

2 Experimental

2.1 Preparation and characterization of as-extruded Mg−Sn−Ca alloys

Pure magnesium (99.98%), pure tin (99.9%) and Mg−30%Ca master alloys were used as starting materials. The nominal composition of Mg−Sn−Ca alloys was that Sn content was varied from 1% to 3% and Ca content from 0.2% to 1.5%. Mg−Sn−Ca alloy ingots were fabricated by induction melting under an atmosphere of high purity argon gas. The stainless steel crucible with the melt was quenched in salt-water solution to obtain the ingot (Sub-rapid solidification process) [24]. The ingots of Mg−Sn−Ca alloys were homogenized at 520 °C for 24 h, followed by quenching in water. The heat-treated ingots were preheated at 380 °C for about 1 h, and then extruded at this temperature with an extrusion ratio of 25:1 to bars of 16 mm in diameter. Chemical compositions of the as-extruded Mg−Sn−Ca alloys were analyzed by an X-ray fluorescence (XRF) analyzer and given in Table 1. According to their nominal composition, the as-extruded Mg−Sn−Ca alloys were named as Mg−1Sn−0.2Ca, Mg−1Sn−0.5Ca, Mg−1Sn−1.5Ca, Mg−2Sn−0.5Ca and Mg−3Sn−0.5Ca, respectively. Rectangular samples with the dimensions of 10 mm × 10 mm × 2 mm were made for the microstructure characterization and immersion test. All samples were ground with SiC paper up to 1000 grit, ultrasonically cleaned in ethanol and dried in cold air.

Table 1 Chemical composition of as-extruded Mg−Sn−Ca alloys

Alloy	*w*/%		
	Sn	Ca	Mg
Mg−1Sn−0.2Ca	1.0209	0.2151	Bal.
Mg−1Sn−0.5Ca	0.9230	0.5072	Bal.
Mg−1Sn−1.5Ca	0.9478	1.4985	Bal.
Mg−2Sn−0.5Ca	1.9312	0.4899	Bal.
Mg−3Sn−0.5Ca	2.9688	0.5346	Bal.

Optical microscopy and scanning electron microscopy (SEM, TESCAN VEGA II LMU) equipped with an energy dispersive spectrometry (EDX) were used to observe the microstructure of as-extruded Mg−Sn−Ca alloys. X-ray diffraction (XRD) was used to examine the phase, presented in the alloys, using a Rigaku D/MAX−2500PC diffractometer with Cu K_α radiation generated at 40 kV and 30 mA and a scan rate of 2 (°)/min in a 2θ range of 20°−80°. To investigate mechanical properties of the alloys, tensile test was carried out at room temperature on a CMT−5105 electronic universal testing machine with a nominal strain rate of 2×10^{-3} s^{-1}.

2.2 Immersion test

Immersion test was carried out according to ASTMG31−72 at 37 °C, and the ratio of the surface area to the volume of solution was set to 1 cm^2 : 20 mL [25]. Hank's solution was used as immersion medium, and the nominal composition of 1 L Hank's solution was listed as follows: 8.00 g NaCl, 0.40 g KCl, 0.14 g $CaCl_2$, 0.35 g $NaHCO_3$, 0.20 g $MgSO_4\cdot7H_2O$, 0.12 g $Na_2HPO_4\cdot12H_2O$, 0.06 g KH_2PO_4 [26]. The pH value of the solution was recorded during the whole immersion test. After immersion in Hank's solution for 250 h, the change of surface morphologies after immersion was observed using a SEM with EDS. Finally, the surface corrosion products of samples were removed using chromate acid (200 g/L CrO_3+10 g/L $AgNO_3$) to calculate the mass loss rate according to the following equation [27]:

$$R_c=\Delta m/(At) \quad (1)$$

where R_c is the corrosion rate, Δm is the mass loss, A is the initial surface area exposed to the Hank's solution, and t is the immersion time.

2.3 Electrochemical test

A three-electrode electrochemical cell with a sample as the working electrode (1.13 cm^2 of exposed area to Hank's solution), a saturated calomel electrode as the reference electrode and a platinum plate as the counter electrode, was used in the electrochemical test. The potentiodynamic polarization tests were carried out at a scan rate of 1 mV/s, and the set immersion time of open circuit potential (OCP) test was 300 s. The scanning potential ranged from ±300 mV (vs SCE) relative to the

OCP. Electrochemical impedance spectroscopy (EIS) tests were performed using a Gamry Reference 600 instrument. The measuring frequency ranged from 10^5 to 10^{-2} Hz and the amplitude of the sinusoidal potential signal was 5 mV with respect to the OCP.

3 Results and discussion

3.1 Microstructure

Figure 1 illustrated the optical microstructures of the as-extruded Mg−Sn−Ca alloys. It could be found that Mg−1Sn−0.2Ca alloy showed long elongated grains with an inhomogeneous microstructure. A high length of hundreds of micrometers and a high width of tens of micrometers in the largest grains, and the smallest grains were of tens of micrometers in length and several micrometers in width. For Mg−1Sn−*x*Ca alloys, with the increase of Ca content from 0.2% to 0.5%, the microstructure became more homogeneous and the grain size decreased. With further increase in Ca content to 1.5%, no obvious change of microstructure was observed from the optical micrographs. As for Mg−*x*Sn−0.5Ca alloys, with the increase of Sn content from 1% to 2%, the microstructure of Mg−2Sn−0.5Ca alloy became less homogeneous. Further increase in Sn content from 2% to 3% introduced no obvious change of microstructure. Long elongated grains and inhomogeneous microstructure were thought to arise from the incomplete dynamic recrystallization at the extrusion temperature of 380 °C [23,28]. The homogeneous microstructure and fine grain size showed a fully recrystallized microstructure [23]. Based on the observation of optical micrographs, it could be found that the microstructure of the as-extruded Mg−Sn−Ca alloys was influenced by Sn/Ca mass ratio in the present study.

SEM images and EDS spectra of the as-extruded Mg−Sn−Ca alloys were shown in Fig. 2. It could be found that some particles were observed in the as-extruded Mg−Sn−Ca alloys. The particles in the as-extruded Mg−1Sn−0.2Ca, Mg−2Sn−0.5Ca and Mg−3Sn−0.5Ca alloys dispersed randomly in the matrix, while the particles in the as-extruded Mg−1Sn−0.5Ca and Mg−1Sn−1.5Ca alloys homogeneously dispersed in the matrix. EDS analysis on Fig. 2 revealed that in Mg−1Sn−1.5Ca alloy, the large white particle (Fig. 2(f)) contained Sn, Mg and Ca elements, and the large black particle (Fig. 2(g)) contained both Mg and Ca elements.

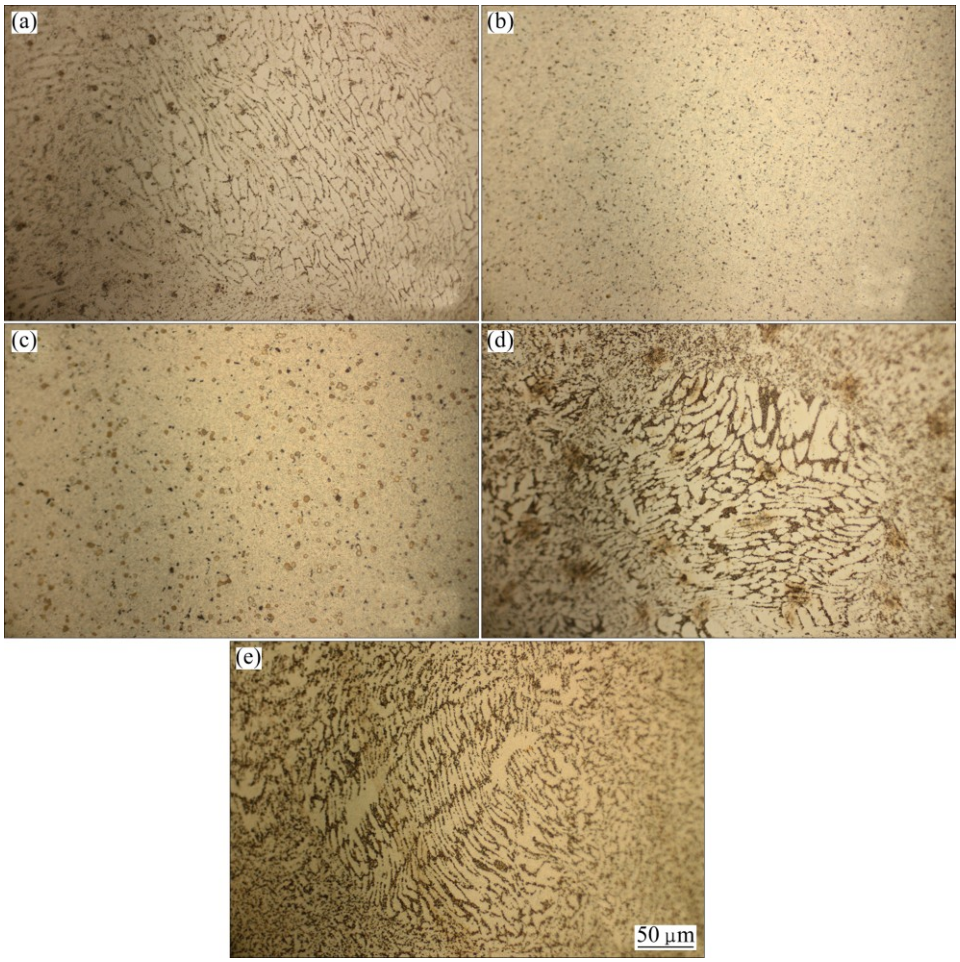

Fig. 1 Optical micrographs of as-extruded Mg−Sn−Ca alloys perpendicular to extruded direction: (a) Mg−1Sn−0.2Ca; (b) Mg−1Sn−0.5Ca; (c) Mg−1Sn−1.5Ca; (d) Mg−2Sn−0.5Ca; (e) Mg−3Sn−0.5Ca

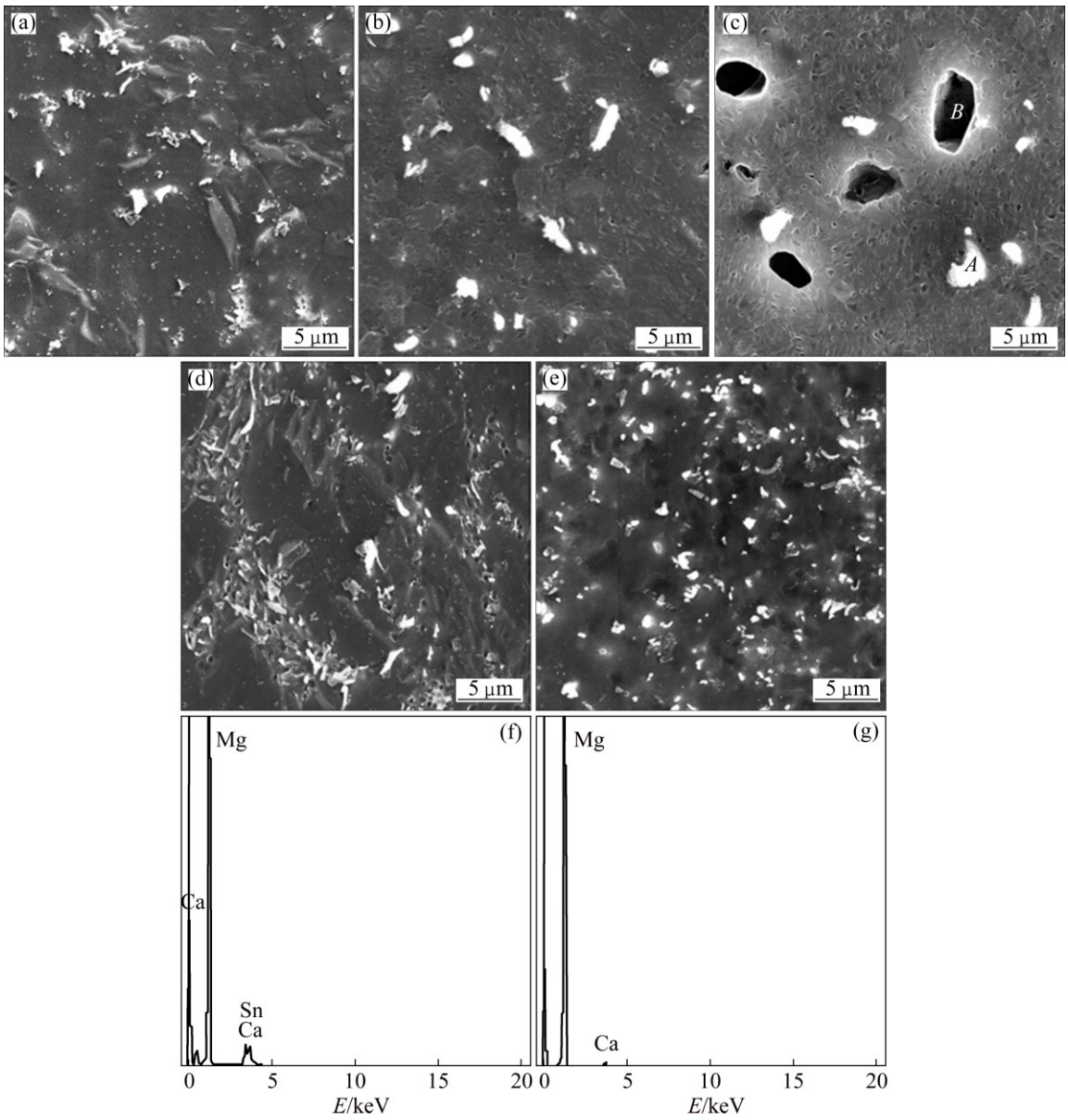

Fig. 2 SEM images (a−e) and EDS spectra (f, g) of as-extruded Mg−Sn−Ca alloys: (a) Mg−1Sn−0.2Ca; (b) Mg−1Sn−0.5Ca; (c) Mg−1Sn−1.5Ca; (d) Mg−2Sn−0.5Ca; (e) Mg−3Sn−0.5Ca; (f) Area *A* in (c); (g) Area *B* in (c)

Figure 3 showed XRD patterns of the as-extruded Mg−Sn−Ca alloys. It could be found that, with the Sn addition of 1%, CaMgSn phase appeared in the as-extruded Mg−1Sn−0.2Ca alloy, and the peak of Mg_2Ca phase became obvious when increasing the Ca content from 0.5% to 1.5%. In Mg−*x*Sn−0.5Ca alloys, the CaMgSn phase was present in all three alloys with the Sn content from 1% to 3%. No peak of Mg_2Sn phase was evidently observed. The results of the SEM/EDS and XRD analyses indicated that the large white particle was CaMgSn phase, the large black particle was Mg_2Ca phase.

It was reported that the Sn/Ca mass ratio decided the phase composition of Mg−Sn−Ca alloys [21,29]. A mass ratio of 3:1 bounds nearly all Ca in forming CaMgSn phase. At mass ratios lower than about 2.5:1,

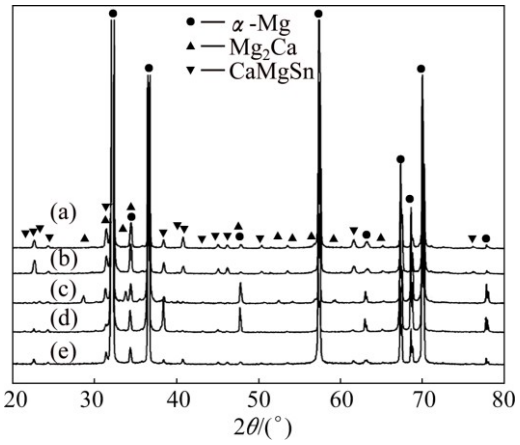

Fig. 3 XRD patterns of as-extruded Mg−Sn−Ca alloys: (a) Mg−3Sn−0.5Ca; (b) Mg−2Sn−0.5Ca; (c) Mg−1Sn−1.5Ca; (d) Mg−1Sn−0.5Ca; (e) Mg−1Sn−0.2Ca

Mg_2Ca phase was formed at grain boundaries, and Mg_2Sn phase appeared at Sn/Ca mass ratios higher than 3:1 [29]. In the present study, Mg−1Sn−0.2Ca, Mg−2Sn−0.5Ca and Mg−3Sn−0.5Ca had Sn/Ca mass ratios higher than 3:1. Therefore, besides forming CaMgSn phase, Mg_2Sn phase, such as small white particle in Fig. 2(e), might be present in the alloy. However, no peaks of Mg_2Sn phase were detected by XRD, as shown in Fig. 3, due to its low fraction. In addition, Mg−1Sn−0.2Ca, Mg−2Sn−0.5Ca and Mg−3Sn−0.5Ca alloys exhibited an inhomogeneous microstructure at Sn/Ca mass ratios higher than 3:1, which were shown in Figs. 1 and 2. On the other hand, Sn/Ca mass ratios in Mg−1Sn−0.5Ca and Mg−1Sn−1.5Ca alloys were lower than 2.5:1, which meant that Mg_2Ca phase should be present in these alloys besides CaMgSn phase. SEM images and XRD patterns (Figs. 2 and 3) confirmed that the Mg_2Ca phase was present in Mg−1Sn−1.5Ca alloy, but Mg_2Ca phase was reluctant to be observed in Mg−1Sn−0.5Ca alloy due to the low content of Mg_2Ca phase.

3.2 Mechanical properties

Tensile properties of the as-extruded Mg−Sn−Ca alloys were demonstrated in Fig. 4. It could be seen that, with the addition of 1% Sn, both the yield strength (YS) and the ultimate tensile strength (UTS) of the as-extruded Mg−Sn−Ca alloys increased when increasing the Ca content from 0.2% to 1.5%. However, the elongation of the alloys increased when the Ca content increased from 0.2% to 0.5%, and decreased when the Ca content was further increased to 1.5%. Grain refinement and the formation of Mg_2Ca second phase were contributed to the improvement of strength [28]. Meanwhile, grain refinement was beneficial to the increase of the ductility. However, excessive Mg_2Ca phase in the as-extruded Mg−1Sn−1.5Ca alloy was detrimental to the ductility [17]. With the addition of 0.5% Ca, the YS and elongation of the as-extruded Mg−Sn−Ca alloys decreased with increasing Sn content from 1% to 2%, and then increased when the Sn content was further increased from 2% to 3%. This result was attributed to the complete transformation of the small amount of Mg_2Ca in the as-extruded Mg−1Sn−0.5Ca alloy to coarse CaMgSn phase in the as-extruded Mg−2Sn−0.5Ca alloy. In addition, the as-extruded Mg−1Sn−0.5Ca alloy had a more homogeneous structure and a lower grain size, which also endowed it with relatively high strength. Compared with the as-extruded Mg−2Sn−0.5Ca alloy, the as-extruded Mg−3Sn−0.5Ca alloy had more Mg_2Sn particles, which contributed to the improvement of YS.

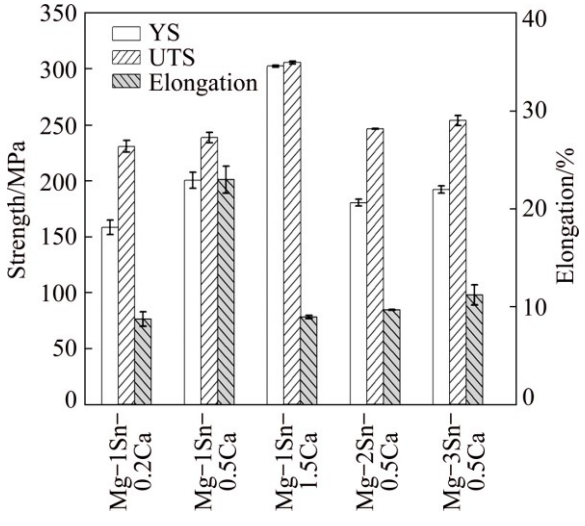

Fig. 4 Mechanical properties of as-extruded Mg−Sn−Ca alloys

3.3 Immersion test

Figure 5 showed the variation of pH values of Hank's solution as a function of immersion time for the as-extruded Mg−Sn−Ca alloys. It could be seen that pH value of Hank's solution corresponding to all as-extruded Mg−Sn−Ca alloys increased rapidly in the initial 24 h, and increased slowly afterward. During the immersion, pH values of Hank's solution for the as-extruded Mg−Sn−Ca alloys at the same time increased in the order of Mg−1Sn−0.5Ca, Mg−2Sn−0.5Ca, Mg−3Sn−0.5Ca, Mg−1Sn−0.2Ca and Mg−1Sn−1.5Ca. pH values of Hank's solution corresponding to Mg−2Sn−0.5Ca, Mg−3Sn−0.5Ca and Mg−1Sn−0.2Ca were close at each time.

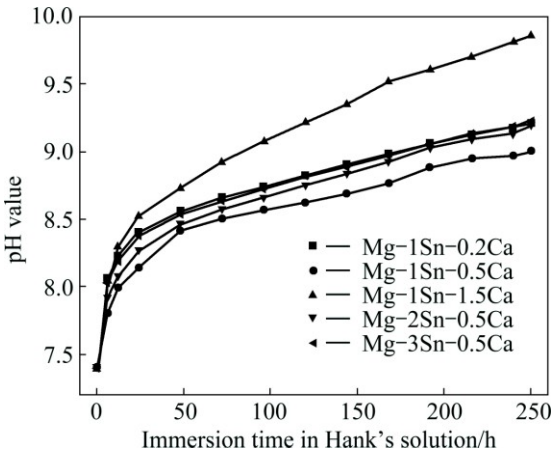

Fig. 5 Variation of pH value of Hank's solution as function of immersion time for as-extruded Mg−Sn−Ca alloys

The corrosion of Mg alloys occurred after immersion in Hank's solution according to the following equation [13]:

$$Mg+2H_2O=Mg(OH)_2+H_2\uparrow \quad (2)$$

It was believed that the accumulation of OH^- ion in the form of $Mg(OH)_2$ on the surfaces of Mg alloys was attributed to the primary increase of pH value of Hank's

solution, and the pH variation trend could reveal the corrosion resistance of Mg alloys [13,30]. Therefore, according to the pH variation trend shown in Fig. 5, it was concluded that the as-extruded Mg−1Sn−0.5Ca alloy exhibited the best corrosion resistance while the as-extruded Mg−1Sn−1.5Ca alloy showed the worst one.

Surface morphologies of the as-extruded Mg−Sn−Ca alloys after immersion in Hank's solution for 250 h were shown in Fig. 6. All as-extruded Mg−Sn−Ca alloy samples maintained the structural integrity during the immersion. Surfaces of all samples were covered with corrosion products (Fig. 6). It could be observed that the coverage of the corrosion products gradually increased in the order of Mg−1Sn−0.5Ca, Mg−2Sn−0.5Ca, Mg−3Sn−0.5Ca, Mg−1Sn−0.2Ca and Mg−1Sn−1.5Ca, which indicated that the as-extruded Mg−1Sn−1.5Ca alloys suffered the severest attack during the immersion. When Mg alloys were immersed in Hank's solution, $Mg(OH)_2$ protective film formed on the surface of the sample due to the corrosion [13]. When increasing the pH value (Fig. 5), ions of the Hank's solution such as PO_4^{3-} and Ca^{2+}, were attracted to the surface of the sample, causing the formation of corrosion products [31]. EDS analysis (Figs. 6(f) and (g)) on the corrosion surface of the as-extruded Mg−1Sn−0.5Ca alloy (Fig. 6(b)) showed that many elements, i.e., sodium (Na), carbon (C), oxygen (O), magnesium (Mg), phosphorus (P) and calcium (Ca), were present in the white precipitates. In the black corrosion products, the presence of C, O, Mg, P and Ca elements indicated that the corrosion products might be magnesium/calcium-containing phosphates [31].

Figure 7 showed the average mass loss rate of the as-extruded Mg−Sn−Ca alloys after being immersed in

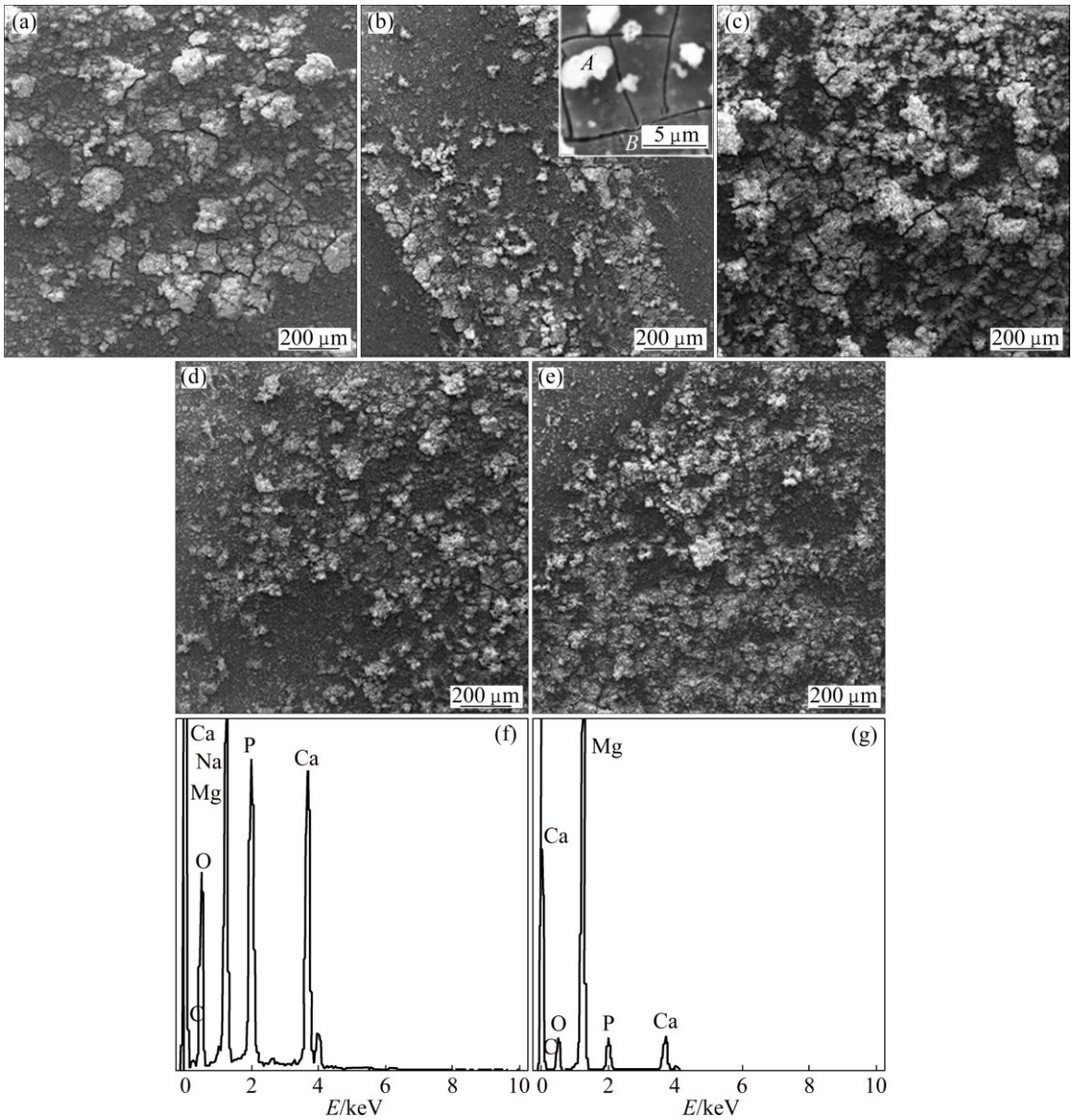

Fig. 6 Surface morphologies (a−e) and EDS spectra (f, g) of as-extruded Mg−Sn−Ca alloys after being immersed in Hank's solution for 250 h: (a) Mg−1Sn−0.2Ca; (b) Mg−1Sn−0.5Ca; (c) Mg−1Sn−1.5Ca; (d) Mg−2Sn−0.5Ca; (e) Mg−3Sn−0.5Ca; (f) Area *A* in (b); (g) Area *B* in (b)

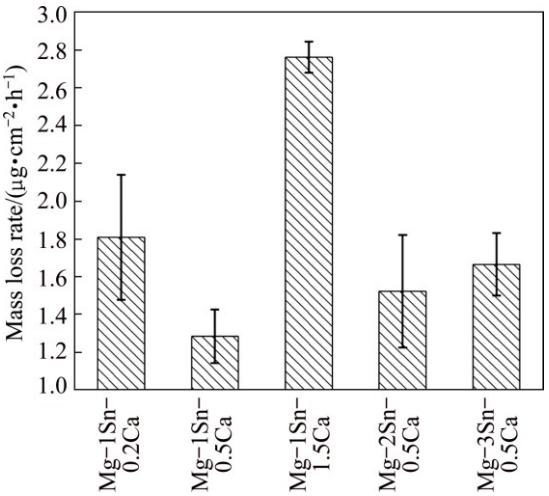

Fig. 7 Average mass loss rate of as-extruded Mg−Sn−Ca alloys after being immersed in Hank's solution for 250 h

Hank's solution for 250 h. It was found that the mass loss rate of the as-extruded Mg−Sn−Ca alloys increased in the order of Mg−1Sn−0.5Ca, Mg−2Sn−0.5Ca, Mg−3Sn−0.5Ca, Mg−1Sn−0.2Ca and Mg−1Sn−1.5Ca. The as-extruded Mg−1Sn−0.5Ca alloy exhibited the best corrosion resistance, while the as-extruded Mg−1Sn−1.5Ca alloy was of the lowest corrosion resistance among the as-extruded Mg−Sn−Ca alloys.

3.4 Electrochemical test

Potentiodynamic polarization curves and EIS spectra of the as-extruded Mg−Sn−Ca alloys in Hank's solution were illustrated in Fig. 8, and the corrosion potential (φ_{corr}) and corrosion current density (J_{corr}) derived from potentiodynamic polarization curves of the as-extruded Mg−Sn−Ca alloys in Hank's solution were listed in Table 2. The results revealed that the J_{corr} increased in the order of Mg−1Sn−0.5Ca, Mg−2Sn−0.5Ca, Mg−3Sn−0.5Ca, Mg−1Sn−0.2Ca and Mg−1Sn−1.5Ca. The results of polarization curves indicated that the as-extruded Mg−1Sn−0.5Ca alloy showed the best corrosion resistance while the as-extruded Mg−1Sn−1.5Ca alloy was the worst one [13]. The results of potentiodynamic polarization tests were in good agreement with those of the immersion tests. The EIS spectra of the as-extruded Mg−Sn−Ca alloys in Hank's solution were shown in Figs. 8(b) and (c). The diameter of the capacitive loop in the Nyquist plots, as well as $|Z|$ of the as-extruded Mg−Sn−Ca alloys, increased in the order of Mg−1Sn−1.5Ca, Mg−1Sn−0.2Ca, Mg−3Sn−0.5Ca, Mg−2Sn−0.5Ca and Mg−1Sn−0.5Ca. The as-extruded Mg−1Sn−0.5Ca alloy showed the best corrosion resistance, as the diameter of the capacitive loop was proportional to the corrosion resistance of materials [32,33]. The results of the EIS tests were in

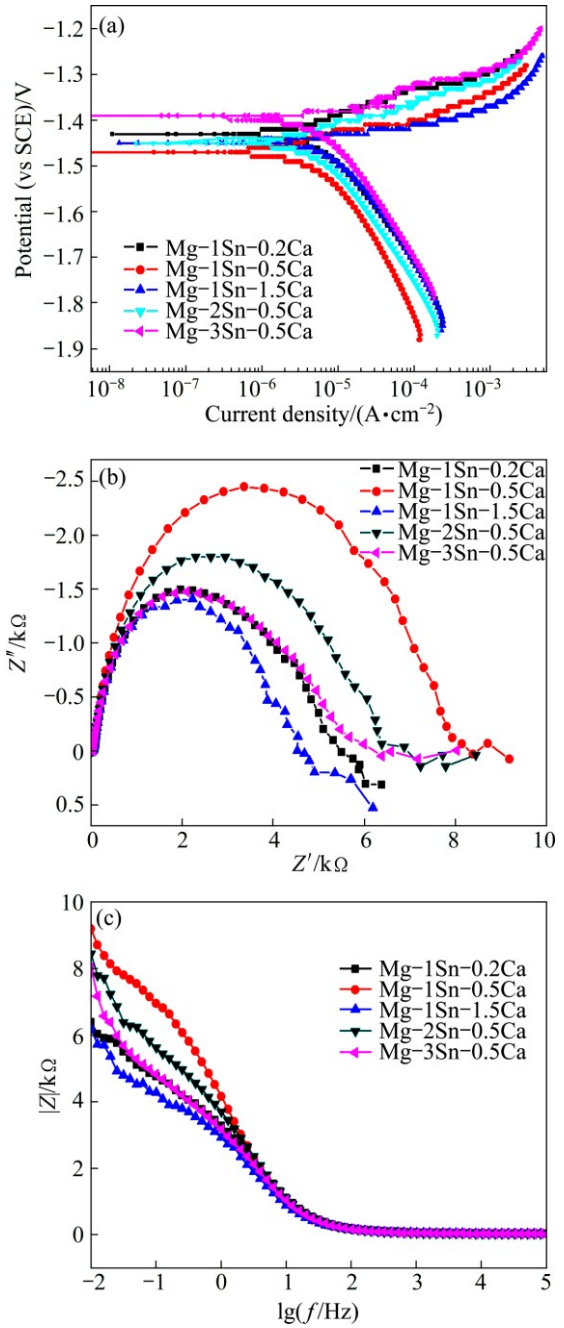

Fig. 8 Potentiodynamic polarization curves and EIS spectra of as-extruded Mg−Sn−Ca alloys in Hank's solution: (a) Potentiodynamic polarization curves; (b) Nyquist plots; (c) Bode plots of $|Z|$ vs frequency

Table 2 Electrochemical parameters derived from potentiodynamic polarization curves of as-extruded Mg−Sn−Ca alloys in Hank's solution

Alloy	φ_{corr} (vs SCE)/V	J_{corr}/(μA·cm^{-2})
Mg−1Sn−0.2Ca	−1.429	6.956
Mg−1Sn−0.5Ca	−1.469	5.950
Mg−1Sn−1.5Ca	−1.449	8.860
Mg−2Sn−0.5Ca	−1.450	6.733
Mg−3Sn−0.5Ca	−1.389	6.844

consistent with those of the immersion tests and potentiodynamic polarization tests.

Many literatures have revealed that low grain size could improve the corrosion properties of Mg alloys [34−36]. In this study, Mg−1Sn−0.5Ca and Mg−1Sn−1.5Ca alloys had lower grain size and homogenous microstructures than the other alloys. According to these literatures, these two alloys would have better corrosion resistance. However, the corrosion resistance of Mg−1Sn−1.5Ca alloy was inferior to those of Mg−1Sn−0.2Ca, Mg−2Sn−0.5Ca and Mg−3Sn−0.5Ca alloys, which was probably related to the difference between second phases of Mg−Sn−Ca alloys. It was reported that second phase could act as galvanic cathodes to accelerate corrosion depending on the anode/cathode area ratio, or act as corrosion barriers to hinder corrosion if it was finely divided and continuous [37, 38]. In this study, second phases, such as CaMgSn phase, Mg_2Ca and Mg_2Sn, might act as cathodes to accelerate corrosion as all reported second phases had more positive corrosion potentials than the α-phase [39], and the second phases herein were not finely divided and continuous. Compared with the CaMgSn phase and Mg_2Sn in Mg−1Sn−0.2Ca, Mg−2Sn−0.5Ca and Mg−3Sn−0.5Ca alloys, Mg_2Ca in Mg−1Sn−1.5Ca alloy might play an important role in deteriorating the corrosion resistance of Mg−Sn−Ca alloys.

According to these investigations, it could be found that in this study, the as-extruded Mg−1Sn−0.5Ca alloy showed a homogenous microstructure, a low degradation rate and good mechanical properties. The good in vitro and in vivo biocompatibility of the alloying element of Ca for orthopedic magnesium alloy implants has been reported [12,16]. A previous study and our recent studies demonstrated good in vitro biocompatibility of alloying element Sn for orthopedic magnesium alloy [10,40,41]. It was therefore believed that the as-extruded Mg−1Sn−0.5Ca alloy was promising as a biodegradable alloy candidate for orthopedic applications.

4 Conclusions

1) For the as-extruded Mg−Sn−Ca alloys, with the addition of 1% Sn, when decreasing the Sn/Ca mass ratio, the homogeneity of the microstructure increased as well as the tensile yield strength and the ultimate tensile strength, and the ductility and corrosion resistance were of the lowest ones at the Sn/Ca mass ratio of 1:1.5. The formation and quantity of Mg_2Ca, besides the CaMgSn phase, played a significant role in the behaviors of the as-extruded Mg−Sn−Ca alloys.

2) For alloys with the addition of 0.5% Ca, when increasing the Sn/Ca mass ratio, the ultimate tensile strength of the as-extruded Mg−Sn−Ca alloys increased with a decreased homogeneity of the microstructure and a decreased corrosion resistance, and the tensile yield strength and the ductility decreased first and then increased slightly. The formation and quantity of Mg_2Sn besides CaMgSn played a significant role in the behaviors of as-extruded Mg−Sn−Ca alloys.

3) The as-extruded Mg−1Sn−0.5Ca alloy had a homogenous microstructure, good mechanical properties and low corrosion rate, and this alloy might be potential for orthopedic applications.

References

[1] LI N, ZHENG Y. Novel magnesium alloys developed for biomedical application: A review [J]. Journal of Materials Science and Technology, 2013, 29(6): 489−502.

[2] STAIGER M P, PIETAK A M, HUADMAI J, DIAS G. Magnesium and its alloys as orthopedic biomaterials: A review [J]. Biomaterials, 2006, 27(9): 1728−1734.

[3] SHAHRI S M G, IDRIS M H, JAFARI H, GHOLAMPOUR B, ASSADIAN M. Effect of solution treatment on corrosion characteristics of biodegradable Mg−Zn alloy [J]. Transactions of Nonferrous Metals Society of China, 2015, 25(5): 1490−1499.

[4] SEYEDRAOUFI Z S, MIRDAMADI S. In vitro biodegradability and biocompatibility of porous Mg−Zn scaffolds coated with nano hydroxyapatite via pulse electrodeposition [J]. Transactions of Nonferrous Metals Society of China, 2015, 25: 4018−4027.

[5] WITTE F, FISCHER J, NELLESEN J, CROSTACK H A, KAESE V, PISCH A, BECKMANN F, WINDHAGEN H. In vitro and in vivo corrosion measurements of magnesium alloys [J]. Biomaterials, 2006, 27(7): 1013−1018.

[6] WITTE F, KAESE V, HAFERKAMP H, SWITZER E, MEYER-LINDENBERG A, WIRTH C, WINDHAGEN H. In vivo corrosion of four magnesium alloys and the associated bone response [J]. Biomaterials, 2005, 26(17): 3557−3563.

[7] WITTE F, FISCHER J, NELLESEN J, VOGT C, VOGT J, DONATH T, BECKMANN F. In vivo corrosion and corrosion protection of magnesium alloy LAE442 [J]. Acta Biomaterialia, 2010, 6(5): 1792−1799.

[8] EL-RAHMAN S S A. Neuropathology of aluminum toxicity in rats (glutamate and GABA impairment) [J]. Pharmacological Research, 2003, 47(3): 189−194.

[9] NAKAMURA Y, TSUMURA Y, TONOGAI Y, SHIBATA T, ITO Y. Differences in behavior among the chlorides of seven rare earth elements administered intravenously to rats [J]. Toxicological Sciences, 1997, 37(2): 106−116.

[10] GU X, ZHENG Y, CHENG Y, ZHONG S, XI T. In vitro corrosion and biocompatibility of binary magnesium alloys [J]. Biomaterials, 2009, 30(4): 484−498.

[11] ILICH J Z, KERSTETTER J E. Nutrition in bone health revisited: A story beyond calcium [J]. Journal of the American College of Nutrition, 2000, 19(6): 715−737.

[12] LI Z, GU X, LOU S, ZHENG Y. The development of binary Mg−Ca alloys for use as biodegradable materials within bone [J]. Biomaterials, 2008, 29(10): 1329−1344.

[13] RAD H R B, IDRIS M H, KADIR M R A, FARAHANY S. Microstructure analysis and corrosion behavior of biodegradable Mg−Ca implant alloys [J]. Materials and Design, 2012, 33: 88−97.

[14] KIM W C, KIM J G, LEE J Y, SEOK H K. Influence of Ca on the corrosion properties of magnesium for biomaterials [J]. Materials Letters, 2008, 62(25): 4146−4148.

[15] WAN Y, XIONG G, LUO H, HE F, HUANG Y, ZHOU X. Preparation and characterization of a new biomedical magnesium−calcium alloy [J]. Materials and Design, 2008, 29(10): 2034−2037.

[16] ERDMANN N, ANGRISANI N, REIFENRATH J, LUCAS A, THOREY F, BORMANN D, MEYER-LINDENBERG A. Biomechanical testing and degradation analysis of MgCa0.8 alloy screws: A comparative in vivo study in rabbits [J]. Acta Biomaterialia, 2011, 7(3): 1421−1428.
[17] ZHANG E, YANG L. Microstructure, mechanical properties and bio-corrosion properties of Mg−Zn−Mn−Ca alloy for biomedical application [J]. Materials Science and Engineering A, 2008, 497(1): 111−118.
[18] SUN Y, ZHANG B, WANG Y, GENG L, JIAO X. Preparation and characterization of a new biomedical Mg−Zn−Ca alloy [J]. Materials and Design, 2012, 34: 58−64.
[19] NIINOMI M. Recent research and development in titanium alloys for biomedical applications and healthcare goods [J]. Science and Technology of Advanced Materials, 2003, 4(5): 445−454.
[20] ZHANG W, LI M, CHEN Q, HU W, ZHANG W, XIN W. Effects of Sr and Sn on microstructure and corrosion resistance of Mg−Zr−Ca magnesium alloy for biomedical applications [J]. Materials and Design, 2012, 39: 379−383.
[21] HORT N, HUANG Y, ABU LEIL T, MAIER P, KAINER K U. Microstructural investigations of the Mg−Sn−*x*Ca system [J]. Advanced Engineering Materials, 2006, 8(5): 359−364.
[22] NAYYERI G, MAHMUDI R. The microstructure and impression creep behavior of cast, Mg−5Sn−*x*Ca alloys [J]. Materials Science and Engineering A, 2010, 527(7): 2087−2098.
[23] ABU LEIL T, HORT N, DIETZEL W, BLAWERT C, HUANG Y, KAINER K, RAO K. Microstructure and corrosion behavior of Mg−Sn−Ca alloys after extrusion [J]. Transactions of Nonferrous Metals Society of China, 2009, 19(1): 40−44.
[24] ZHANG H, ZHANG D, MA C, GUO S. Improving mechanical properties and corrosion resistance of Mg−6Zn−Mn magnesium alloy by rapid solidification [J]. Materials Letters, 2013, 92: 45−48.
[25] ASTM-G31−72. Standard practice for laboratory immersion corrosion testing of metals [S]. Philadelphia, Pennsylvania, USA: American Society for Testing and Materials, 2004.
[26] ZHANG E, YIN D, XU L, YANG L, YANG K. Microstructure, mechanical and corrosion properties and biocompatibility of Mg−Zn−Mn alloys for biomedical application [J]. Materials Science and Engineering C, 2009, 29(3): 987−993.
[27] LIU C, XIN Y, TIAN X, CHU P K. Degradation susceptibility of surgical magnesium alloy in artificial biological fluid containing albumin [J]. Journal of Materials Research, 2007, 22(7): 1806−1814.
[28] ZHANG X, YUAN G, NIU J, FU P, DING W. Microstructure, mechanical properties, biocorrosion behavior, and cytotoxicity of as-extruded Mg−Nd−Zn−Zr alloy with different extrusion ratios [J]. Journal of the Mechanical Behavior of Biomedical Materials, 2012, 9: 153−162.
[29] RAO K, PRASAD Y, SURESH K, HORT N, KAINER K. Hot deformation behavior of Mg−Sn−Ca alloy in as-cast condition and after homogenization [J]. Materials Science and Engineering A, 2012, 552: 444−450.
[30] CAI S, LEI T, LI N, FENG F. Effects of Zn on microstructure, mechanical properties and corrosion behavior of Mg−Zn alloys [J]. Materials Science and Engineering C, 2012, 32(8): 2570−2577.
[31] ZHANG S, ZHANG X, ZHAO C, LI J, SONG Y, XIE C, TAO H, ZHANG Y, HE Y, JIANG Y. Research on an Mg−Zn alloy as a degradable biomaterial [J]. Acta Biomaterialia, 2010, 6(2): 626−640.
[32] BOBBY KANNAN M, SINGH R. A mechanistic study of in vitro degradation of magnesium alloy using electrochemical techniques [J]. Journal of Biomedical Materials Research, 2010, 93(3): 1050−1055.
[33] ZUCCHI F, GRASSI V, FRIGNANI A, MONTICELLI C, TRABANELLI G. Electrochemical behaviour of a magnesium alloy containing rare earth elements [J]. Journal of Applied Electrochemistry, 2006, 36(2): 195−204.
[34] RALSTON K, BIRBILIS N. Effect of grain size on corrosion: A review [J]. Corrosion, 2010, 66(7): 075005−075005-13.
[35] AUNG N N, ZHOU W. Effect of grain size and twins on corrosion behaviour of AZ31B magnesium alloy [J]. Corrosion Science, 2010, 52(2): 589−594.
[36] ARGADE G, PANIGRAHI S, MISHRA R. Effects of grain size on the corrosion resistance of wrought magnesium alloys containing neodymium [J]. Corrosion Science, 2012, 58: 145−151.
[37] SONG G, ATRENS A, DARGUSCH M. Influence of microstructure on the corrosion of diecast AZ91D [J]. Corrosion Science, 1998, 41(2): 249−273.
[38] ZHAO M C, LIU M, SONG G, ATRENS A. Influence of the β-phase morphology on the corrosion of the Mg alloy AZ91 [J]. Corrosion Science, 2008, 50(7): 1939−1953.
[39] SONG G, ATRENS A. Understanding magnesium corrosion-framework for improved alloy performance [J]. Advanced Engineering Materials, 2003, 5(12): 837−858.
[40] ZHAO C, PAN F, ZHAO S, PAN H, SONG K, TANG A. Preparation and characterization of as-extruded Mg−Sn alloys for orthopedic applications [J]. Materials and Design, 2015, 70: 60−67.
[41] ZHAO C, PAN F, ZHAO S, PAN H, SONG K, TANG A. Microstructure, corrosion behavior and cytotoxicity of biodegradable Mg−Sn implant alloys prepared by sub-rapid solidification [J]. Materials Science and Engineering C, 2015, 54: 245−251.

挤压态 Mg−Sn−Ca 合金的显微组织、力学及生物腐蚀性能

赵朝勇[1]，潘复生[1,2,3]，潘虎成[4]

1. 重庆大学 材料科学与工程学院，重庆 400044；
2. 重庆大学 国家镁合金材料工程技术研究中心，重庆 400044；
3. 重庆市科学技术研究院，重庆 401123；
4. 东北大学 材料各向异性与织构教育部重点实验室，沈阳 110819

摘 要：制备了用于骨科的挤压态 Mg−Sn−Ca 合金，并应用金相显微镜、扫描电子显微镜、X 射线衍射仪、拉伸测试、浸泡测试和电化学测试等仪器和方法对其进行研究。结果表明：当锡添加量为 1%，钙含量从 0.2%增加到 0.5%时，挤压态 Mg−Sn−Ca 合金的显微组织变得均匀，力学性能增加，耐腐蚀性提高。钙含量进一步增加到 1.5%时，合金的强度增加，但伸长率和耐腐蚀性降低。在钙含量为 0.5%的合金中，锡的含量从 1%增加到 3%时，合金的最大抗拉强度增加，耐腐蚀性降低。当锡含量为 2%时，合金呈现最低的屈服强度和伸长率。挤压态 Mg−Sn−Ca 合金的这些行为受到 Sn/Ca 比率的控制。分析表明挤压态 Mg−1Sn−0.5Ca 合金有潜力作为可降解骨科植入体。

关键词：镁合金；Mg−Sn−Ca 合金；生物可降解性；骨科植入体；显微组织；力学性能；腐蚀

(Edited by Xiang-qun LI)